# Brief Introduction to Rydberg Atom Array

Yujiang He

Last updated: June 7, 2024

## Contents

# 1 Single-Bit gate

## 1.1 clock state

The quantum information is stored in the clock state of the $Rb^{87}$ atom that is the hyperfine ground states:

The value electron is in the $5S_{1/2}$ state, and the nuclear spin is in the $F = \frac{3}{2}$ state.
Combing the electron and nuclear spin, the total angular momentum is $\boldsymbol{F} = \boldsymbol{I} + \boldsymbol{J} + \boldsymbol{S}$. We encode qubits as:

$$\begin{aligned} |0\rangle &= |5S_{1/2}, F = 1, m_F = 0\rangle \\ |1\rangle &= |5S_{1/2}, F = 2, m_F = 0\rangle \end{aligned} \tag{1}$$

## 1.2 Single-bit rotation

The single-bit rotation is realized by the microwave field. The Hamiltonian is:

$$H(t) = H_0 + H_I(t) = \begin{pmatrix} \omega_a & 0 \\ 0 & \omega_b \end{pmatrix} + \begin{pmatrix} 0 & \Omega\cos(\omega t + \phi) \\ \Omega^* \cos(\omega t + \phi) & 0 \end{pmatrix} \tag{2}$$

where we choose the unit $\hbar = 1$, $\omega_a$ and $\omega_b$ are the energy of the qubit state $|0\rangle$ and $|1\rangle$, $\Omega$ is the Rabi frequency, $\omega$ is the microwave frequency, and $\phi$ is the phase of the microwave field.

To get the evolution of the qubit state, we can solve the Schrödinger equation in the interacting picture: We can define the new wave function as:

$$|\tilde{\psi}(t)\rangle = e^{iH_0 t} |\psi(t)\rangle \tag{3}$$

Then the Schrödinger equation is:

$$\begin{aligned} i\frac{d}{dt}|\tilde{\psi}(t)\rangle &= i(iH_0)|\tilde{\psi}(t)\rangle + e^{iH_0 t}\left(i\frac{d}{dt}|\tilde{\psi}(t)\rangle\right) \\ &= -H_0|\tilde{\psi}(t)\rangle + e^{iH_0 t}(H_0 + H_I(t))e^{-iH_0 t}|\tilde{\psi}(t)\rangle \\ &= e^{iH_0 t} H_I e^{-iH_0 t}|\tilde{\psi}(t)\rangle \\ Since: cos(\omega t + \phi) &= \frac{1}{2}(e^i(\omega t + \phi) + e^{-i(\omega t + \phi)}) \\ &= \begin{pmatrix} 0 & \frac{\Omega}{2}e^{i(\omega_a - \omega_b)t}(e^{-i(\omega t - \phi)} + e^{i(\omega t - \phi)}) \\ h.c. & 0 \end{pmatrix}|\tilde{\psi}(t)\rangle \end{aligned}$$

Simpfying the equation, we can get the envolving matrix:($Since: cos(\omega t + \phi) = \frac{1}{2}(e^i(\omega t + \phi) + e^{-i(\omega t + \phi)})$)

$$\begin{aligned} e^{iH_0 t} H_I e^{-iH_0 t} &= \begin{pmatrix} 0 & \frac{\Omega}{2}e^{i(\omega_a - \omega_b)t}(e^{-i(\omega t - \phi)} + e^{i(\omega t - \phi)}) \\ h.c. & 0 \end{pmatrix} \\ Using\ the\ condition: \omega_a - \omega_b &= \omega \\ &= \begin{pmatrix} 0 & \frac{\Omega}{2}e^{i\phi} + \frac{\Omega}{2}e^{-i\phi - 2i\omega t} \\ h.c. & 0 \end{pmatrix} \\ Rotating\ wave\ approximation: &\ neglecting\ the\ fast\ rotating\ term \\ &= \begin{pmatrix} 0 & \frac{\Omega}{2}e^{i\phi} \\ h.c. & 0 \end{pmatrix} \end{aligned}$$

## 1.3 Rydberg state

Rydberg atoms are highly excited atoms with a very large principal quantum number $n$. The size of their electron cloud is proportional to $n^2$. The interaction between two Rydberg atoms is extremely strong, shown in fig.1 and fig.2, which will cause Rydberg blockade effect. If we bring two $Rb^{87}$ atoms close enough, only one of them can be excited to the Rydberg state which can be used to realize $CZ$ gate. Also, if three or more atoms are close enough which means they all in the blockade radius, we can use Rydberg blockade to realize $C^nZ$ gate. But our ability to control the atom and the Rydberg blockade radius is limited, the fidelity of the $C^nZ$ gate may decrease with $n$ growing.

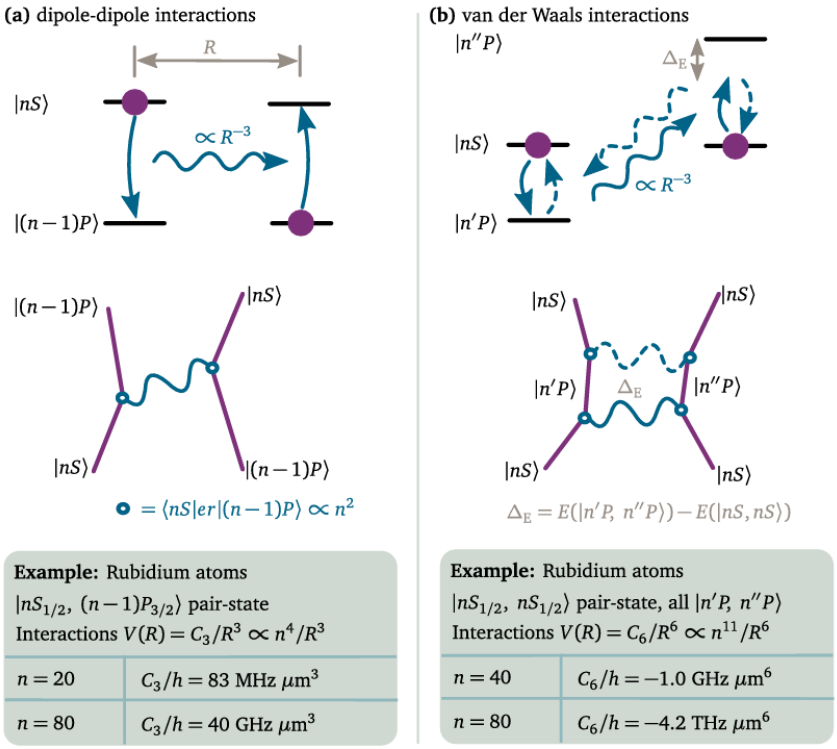


Figure 1: A brief introduction of the interaction between Rydberg atoms, Van der Waals interaction is shown in the Apendix.

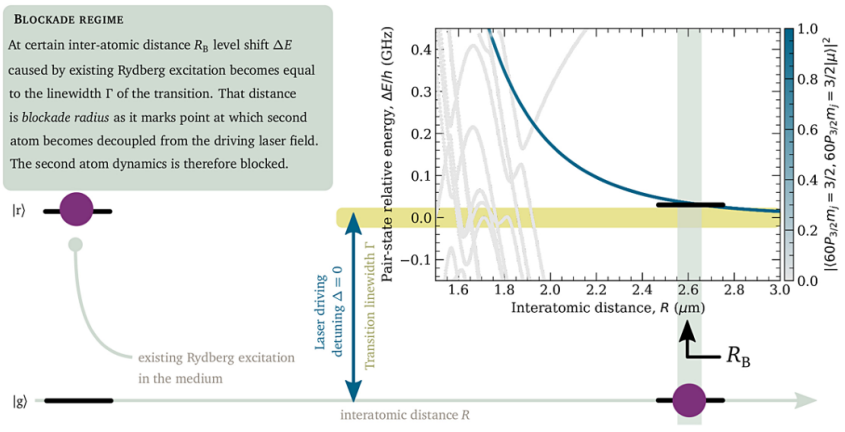


Figure 2: Rydberg blockade effect.

# 2 Two-bit gate

In this section, please allow me to introduce the two-bit gate first, then we will introduce two-photon Rydberg excitation in detail.

## 2.1 The realization of CZ gate

Just like the section 1.2, we can use the microwave field to realize the transfer from $|1\rangle$ to $|r\rangle$. Before explaining the mechanism of this transfermation, we can consider it as a effective two level transfermation.

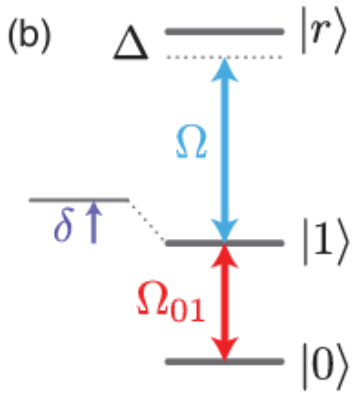


Figure 3: a schematic diagram of the two-level transfermation from $|1\rangle$ to $|r\rangle$.

We can write the Hamiltonian of the two-level system as (in the basis of $\{|1\rangle, |r\rangle\}$): :

$$H = \begin{pmatrix} 0 & \Omega/2 \\ \Omega^*/2 & \Delta \end{pmatrix} \tag{4}$$

where $\Omega$ is the Rabi frequency times phase parameter $e^{i\phi}$, $\Delta$ is the detuning of the microwave field.

Based on the Hamiltonian above, we can write the Hamiltonian of the two-bit system as(in the basis of $\{|11\rangle, |1r\rangle, |r1\rangle, |rr\rangle\}$):

$$H = \begin{pmatrix} 0 & \Omega/2 & \Omega/2 & 0 \\ \Omega^*/2 & \Delta & 0 & \Omega/2 \\ \Omega^*/2 & 0 & \Delta & \Omega/2 \\ 0 & \Omega^*/2 & \Omega^*/2 & 2\Delta + V_{rr} \end{pmatrix} \tag{5}$$

where $V_{rr}$ is the interaction between two Rydberg atoms.($V_{rr} \gg \Omega, \Delta$) In the early reasearch [4], the authors use the parameters $\Omega \approx 2\pi \times 3.5MHz$, $\Delta \approx 0.377\Omega$ to realize the CZ gate with the $V_{rr} \approx 2\pi \times 24MHz \gg \Omega$. Since the term $2\Delta + V_{rr}$ is too large compared with the other terms which means get to $|rr\rangle$ is too hard, we can simplify the Hamiltonian:(in the basis of $\{|11\rangle, |1r\rangle, |r1\rangle\}$)

$$H = \begin{pmatrix} 0 & \Omega/2 & \Omega/2 \\ \Omega^*/2 & \Delta & 0 \\ \Omega^*/2 & 0 & \Delta \end{pmatrix} \tag{6}$$

Now, let's consider the Hamiltonian above in anther basis $\{|a\rangle = |11\rangle, |b\rangle = \frac{1}{\sqrt{2}}(|1r\rangle + |r1\rangle),$

$|c\rangle = \frac{1}{\sqrt{2}}(|1r\rangle - |r1\rangle)\}$, the interacting term will be:

$$\langle c| H |a\rangle = 0, \langle c| H |b\rangle = 0, \langle c| H |c\rangle = \Delta$$
$$\langle b| H |a\rangle = \frac{\sqrt{2}}{2}\Omega, \langle b| H |b\rangle = \Delta, \langle b| H |c\rangle = 0$$

The Hamiltonian in the basis $\{|a\rangle, |b\rangle, |c\rangle\}$ is:

$$H = \begin{pmatrix} 0 & \frac{\sqrt{2}}{2}\Omega & 0 \\ \frac{\sqrt{2}}{2}\Omega & \Delta & 0 \\ 0 & 0 & \Delta \end{pmatrix} \tag{7}$$

Based on the proof above, the $|c\rangle$ state is not allowed. In this case, we can consider this process as two-level system with effective Rabi frequency $\sqrt{2\Omega^2 + \Delta^2}$. The effective frequency of the other initial states is $\sqrt{\Omega^2 + \Delta^2}$.

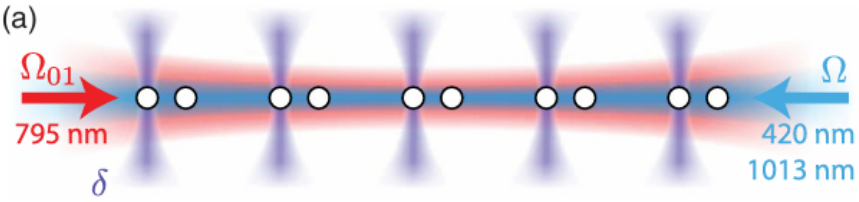


Figure 4: The atoms are controlled by optical tweezers and are excited by a bichromatic Laser globally.

The desired unitary CZ gate maps the computational basis states as follow:

$$|00\rangle \rightarrow |00\rangle$$
$$|01\rangle \rightarrow |01\rangle e^{i\phi}$$
$$|10\rangle \rightarrow |10\rangle e^{i\phi}$$
$$|11\rangle \rightarrow |11\rangle e^{i(2\phi-\pi)}$$

This map is equivalent to the CZ gate up to a single-bit phase $\phi$.

For a chosen detuning $\Delta$, we select the pulse length $\tau$ such that the first laser pulse completes a full cycle of a detuned Rabi oscillation for $|11\rangle$ system. The same pulse drives an incomplete Rabi oscillation on the $|01\rangle$ system. A subsequent phase jump $\Omega \rightarrow \Omega e^{i\xi}$ rotates the orientation of the drive field around the Z axis by an angle $\xi$ such that a second pulse of length $\tau$ completes the oscillation and returns the state to $|01\rangle$ while driving a second complete detuned oscillation on the $|11\rangle$ configuration. By the end of the second pulse, both $|01\rangle$ and $|11\rangle$ return to their initial position on the Bloch sphere but with accumulated dynamical phases $\phi_{01}$ and $\phi_{11}$, which depend on the geometric surface area of Bloch sphere enclosed by the $\Delta$-dependent trajectories. For a specific choice of laser detuning ($\Delta \approx 0.377\Omega$),$2\phi_{01} - \pi = \phi_{11}$, realizing the CZ gate.

Lukin group have reached a fidelity of 96.5% for CNOT gate meausred on the Bell state in August 2019. They have improved the method to realize a better oscillation between $|1\rangle$ and $|r\rangle$ which makes they get high-parallel CZ gate with a fidelity of 99.5% in April 2023, over the break-even point of quantum error correction.

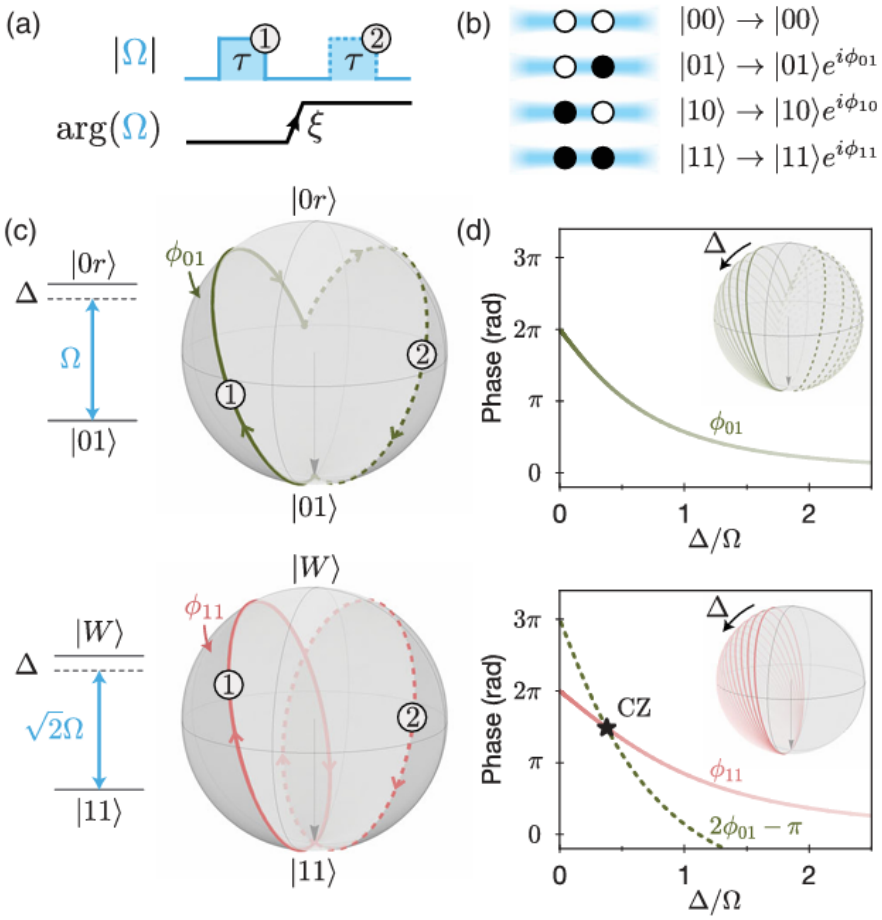


Figure 5: Controlled-phase (CZ) gate protocol.

Using one more $Rb^{87}$ atom, we can realize $CCZ$ gate, shown in fig.6.

The process of the $C^nZ$ gate can be considered as: if a $|1\rangle$ is be excited to $|r\rangle$ and then turn back to $|1\rangle$, it will get a cummutative phase $-1$.

$CZ$ gate:

$$\begin{aligned}\hat{U}_{CZ}|00\rangle &= |00\rangle \\ \hat{U}_{CZ}|01\rangle &= -|01\rangle \\ \hat{U}_{CZ}|10\rangle &= -|10\rangle \\ \hat{U}_{CZ}|11\rangle &= -|11\rangle\end{aligned} \tag{8}$$

Matrix form:

$$\hat{U}_{CZ} = \begin{pmatrix} 1 & 0 & 0 & 0 \\ 0 & -1 & 0 & 0 \\ 0 & 0 & -1 & 0 \\ 0 & 0 & 0 & -1 \end{pmatrix} \tag{9}$$

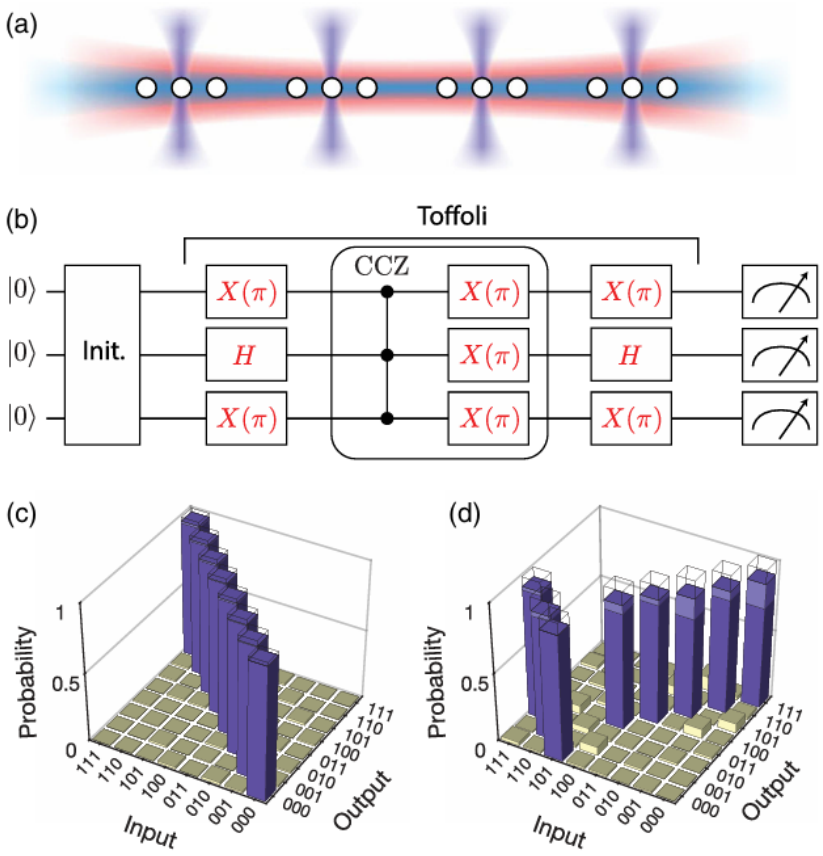


Figure 6: Realization of three-qubit Toffoli gate.[4] Lukin group reached Toffoli gate with the fidelity of 87.0% in 2019, and $CCZ$ gate with the fidelity of 97.9% in 2023.

$CCZ$ gate:

$$\begin{aligned}
\hat{U}_{CCZ}\left|000\right\rangle &= \left|000\right\rangle \\
\hat{U}_{CCZ}\left|001\right\rangle &= -\left|001\right\rangle \\
\hat{U}_{CCZ}\left|010\right\rangle &= -\left|010\right\rangle \\
\hat{U}_{CCZ}\left|011\right\rangle &= -\left|011\right\rangle \\
\hat{U}_{CCZ}\left|100\right\rangle &= -\left|100\right\rangle \\
\hat{U}_{CCZ}\left|101\right\rangle &= -\left|101\right\rangle \\
\hat{U}_{CCZ}\left|110\right\rangle &= -\left|110\right\rangle \\
\hat{U}_{CCZ}\left|111\right\rangle &= -\left|111\right\rangle
\end{aligned} \tag{10}$$

Matrix form:

$$\hat{U}_{CCZ} = \begin{pmatrix}
1 & 0 & 0 & 0 & 0 & 0 & 0 & 0 \\
0 & -1 & 0 & 0 & 0 & 0 & 0 & 0 \\
0 & 0 & -1 & 0 & 0 & 0 & 0 & 0 \\
0 & 0 & 0 & -1 & 0 & 0 & 0 & 0 \\
0 & 0 & 0 & 0 & -1 & 0 & 0 & 0 \\
0 & 0 & 0 & 0 & 0 & -1 & 0 & 0 \\
0 & 0 & 0 & 0 & 0 & 0 & -1 & 0 \\
0 & 0 & 0 & 0 & 0 & 0 & 0 & -1
\end{pmatrix} \tag{11}$$

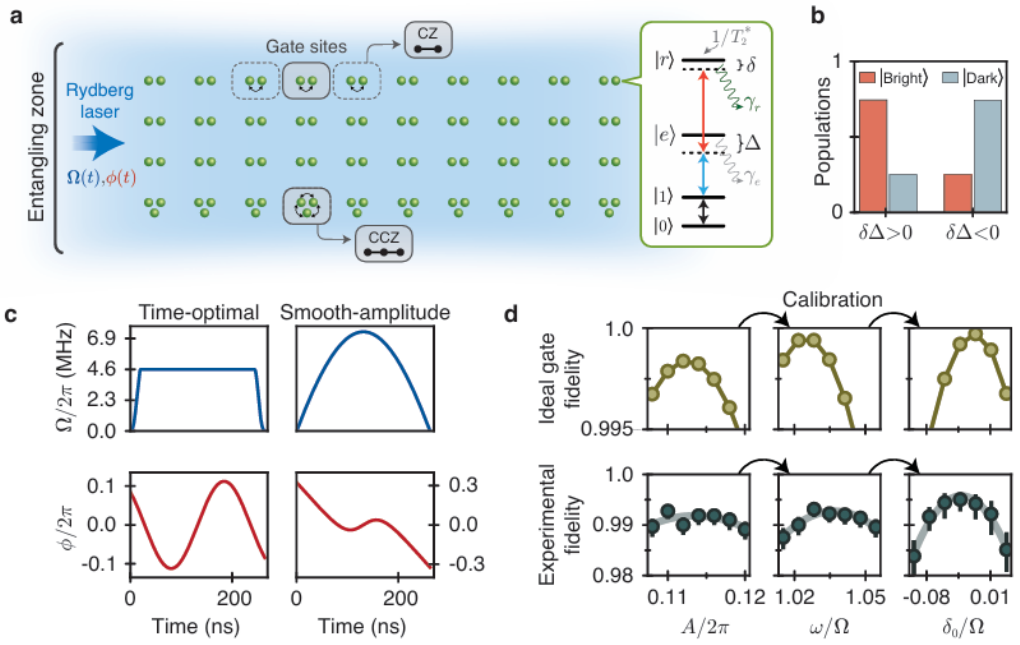


Figure 7: The schematic diagram of the two-photon Rydberg excitation. Main gate error sources include Rydberg state decay $\gamma_r$, intermediate-state scattering $\gamma_e$ (spontaneous emission), and Rydberg dephasing $T_2^*$

## 2.2 two-photon Rydberg excitation

The process discussed in the last subsection all based on the realization of a well performed effective Rabi oscillation between $|1\rangle$ and $|r\rangle$. In this subsection, we will introduce the two-photon Rydberg excitation and how to improve the fidelity of this process[2]. In particular, two-qubit gate error rates below 1% (fidelity above 99%) are required to supass quantum error-correcting thresholds.

There exists four main error sources: Rydberg decay, coupling to the other Rydberg $m_J$ level, intermediate-state scattering, and their measured ground-Rydberg $T_2^* = 3\mu s$ which is dominated by laser light shift fluctuations and finite atomic temperature.

Nowadays, Lukin group have generalized the early time-optimal single laser pluse excitation[3] to time-optimal two laser pluse excitation. They also realized a new method to decrease the intermediate-state scattering, namely smooth-amplitude two laser pulse gate. [2] They further optimize their control pulses to suppress scattering from the short-lived intermediate state $|e\rangle$ by minimizing population in the "bright" dressed state ($|B\rangle \sim |1\rangle + \sqrt{\frac{2\Omega}{\Delta}}|e\rangle + |r\rangle$) containing $|e\rangle$ and maximizing population in the "dark" state ($|D\rangle \sim -|1\rangle + |r\rangle$) not containing $|e\rangle$ (where $\Omega$ is the two-photon Rabi frequency and $\Delta$ is the intermediate-state detuning).

Something improved comparing the early work of Lukin group: They chose to operate at $n = 53$ for benefiting from 50% increase in the Rabi frequency compared to previously used $n = 70$. With more powerful 1013nm laser, they can operate at the intermediate-state detuning of $\Delta/2\pi = 7.8GHz$ with a Rabi frequency of $\Omega/2\pi = 4.6MHz$

### 2.2.1 Dark,Bright state in two-photon Rydberg excitation

The basic intuition can be developed at the single-particle level, where the system is described by the three-level Hamiltonian in the $|1\rangle, |e\rangle, |r\rangle$ basis,

$$H = \begin{pmatrix} 0 & \Omega_b/2 & 0 \\ \Omega_b & -\Delta & \Omega_r/2 \\ 0 & \Omega_r/2 & -\delta \end{pmatrix} \tag{12}$$

where we use symbols $\Omega_b := \Omega_{420}$ and $\Omega_r := \Omega_{1013}$ in this section for clarity of expressions. We also assume that the amplitude and phase of the red 1013-nm laser are kept constant at all times and the blue 420-nm phase is captured by the time-dependent two-photon detuning $\delta := \delta(t) \sim -\phi'(t)$.

At large intermediate detunings ($|\Delta| \gg |\delta|, |\Omega_{b,r}|$), this system is conveniently described in the dark,bright-state basis. We can consider $\delta = 0$, and the eigenstates of the Hamiltonian above can write down to the leading order in $\Omega_r/\Delta$:

$$\begin{aligned} |D\rangle &= -\frac{1}{\sqrt{1+\alpha^2}}|1\rangle + \frac{\alpha}{\sqrt{1+\alpha^2}}|r\rangle, \\ |B\rangle &= \frac{\alpha}{\sqrt{1+\alpha^2}}|1\rangle + \frac{\sqrt{1+\alpha^2}}{2\Delta}|e\rangle + \frac{1}{\sqrt{1+\alpha^2}}|r\rangle, \\ |E\rangle &= -\frac{\alpha\Omega_r}{2\Delta}|1\rangle + |e\rangle - \frac{\Omega_r}{2\Delta}|r\rangle \end{aligned}$$

where $\alpha = \Omega_b/\Omega_r$. Note that the "dark state" $|D\rangle$ has no contribution from the intermediate state, the "bright state" $|B\rangle$ populates from the intermediate state $\approx 1/\Delta^2$, and the state $|E\rangle$ is composed essentially entirely from $|e\rangle$

For our purpose the initial state is always $|1\rangle$, which is subsequently dressed by the blue light to $|\tilde{1}\rangle$. This is because the amplitude rise time of the blue laser to its initial value of $\Omega_b(0)$ is at the timescale of 10ns, which is much slower than the adiabaticity limit set by $\Delta$, and much faster than the two-photon Rabi frequency relevant for populating the Rydberg state; thus, the initial state indeed corresponds to:

$$\begin{aligned} |\tilde{1}\rangle &= |1\rangle + \frac{\alpha\Omega_r}{2\Delta}|e\rangle \\ &= \frac{\alpha}{\sqrt{1+\alpha^2}}|B\rangle - \frac{1}{\sqrt{1+\alpha^2}}|D\rangle + \mathcal{O}(\Delta^{-3})|E\rangle \end{aligned} \tag{13}$$

which is well supported on the $|D\rangle, |B\rangle$ states alone. Moreover, the excited state $|E\rangle$ is detuned from the other two by $\Delta$, and all direct coupling to it are on the order of $\Omega_r/\Delta$; thus any population transfer out of the $|D\rangle, |B\rangle$ manifold will be suppressed by $(\Omega_r\delta)^2/\Delta^4$, and the subsequent evolution of state $|\tilde{1}\rangle$ is described by an effective two-level system.

Example: we can consider the case of the parameterized time-optimal gate where the blue Rabi frequency is kept constant throught the duration of the gate ($\alpha(t) = 1$), up to the finite rise and fall time. The initial state will be $(|D\rangle - |B\rangle)/\sqrt{2}$ and the Hamiltonian will be:

$$\tilde{H} = \begin{pmatrix} 0 & -\delta/2 \\ -\delta/2 & \frac{\Omega_r^2}{2\Delta} \end{pmatrix} \tag{14}$$

with fixed detuning $\delta$ and $\Omega_r$.

The time evolution under this Hamiltonian can be solved exactly, the population in the dark state is:

$$P_D(t) = \frac{1}{2} - \delta\Delta\frac{\Omega_r^2 sin^2(\frac{\sqrt{4\delta^2\Delta^2+\Omega_r^4}}{4\Delta}t)}{2\delta^2\Delta^2+\Omega_r^4} \tag{15}$$

which can go above or below 1/2 depending on the relative sign of the detunings. As expected, one of the trajectories realizes the Rydberg population through the dark state and as a result

minimizes the intermediate-state population, leading to suppressed scattering. The remaining scattering comes mostly from the large admixture of the bright state in the initial state and can be further reduced by utilizing a smooth amplitude profile, which starts at low blue Rabi frequency ($\alpha \ll 1$) and only later increases to larger values, as is the case of adiabatic passage.

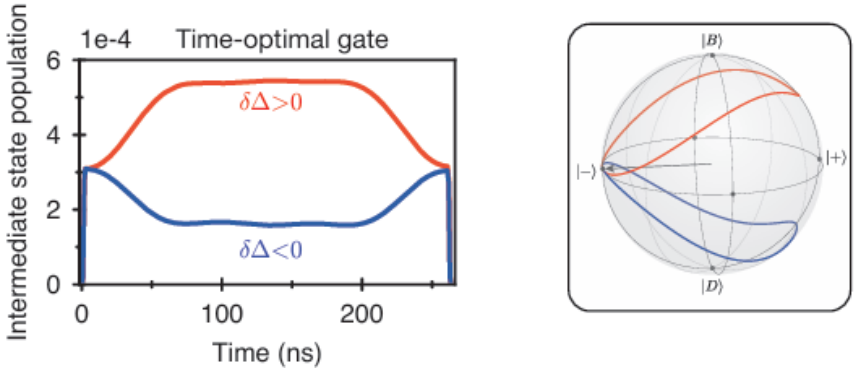


Figure 8: intermediate-state population during the parameterized time-optimal gate in the dark and bright configuration together with their Bloch sphere trajectories in the $|D\rangle, |B\rangle$ basis.

The Hamiltonianof the bare atomic system and the effective two-level system, where $\alpha$ is the time-dependent ratio between the blue and red Rabi frequency and $\dot{\alpha}$ is its time derivative.

$$\tilde{H} = \begin{pmatrix} -\frac{\alpha^2\delta}{1+\alpha^2} & -\frac{\alpha\delta - i\dot{\alpha}}{1+\alpha^2} \\ -\frac{\alpha\delta + i\dot{\alpha}}{1+\alpha^2} & -\frac{\delta}{1+\alpha^2} + \frac{(\alpha^2+1)\Omega^2}{4\Delta} \end{pmatrix} \tag{16}$$

which is expressed in the $|D\rangle, |B\rangle$ basis.

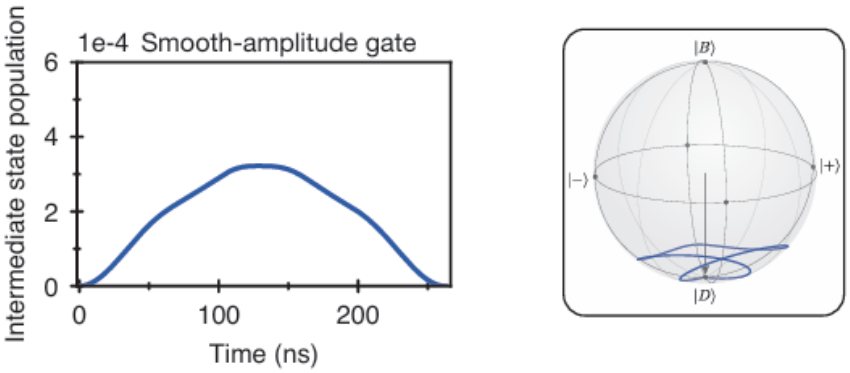


Figure 9: Intermediate-state population during the smooth-amplitude gate and its Bloch sphere trajectory in the instantaneous

# A Van der Waals interaction

Considering two neutral atoms, there is a weak attraction between them if they are polarizable. To model this system, picture each atom as an electron (mass m, charge -e) attached by a spring (spring constant k) to a nucleus (charge +e).

Assume: nuclei are heavy and essentially motionless.

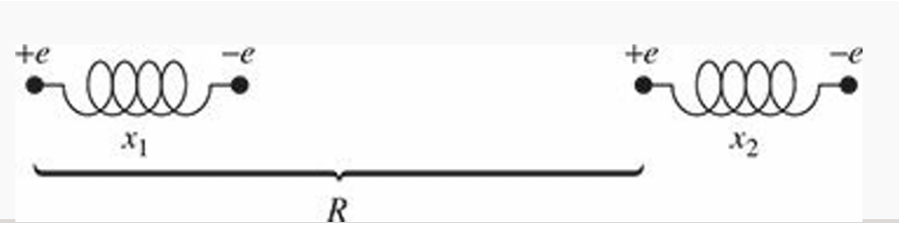


Figure 10: Schematic diagram of the Van der Waals interaction

The Hamiltonian of the unperturbed system is:

$$H_0 = \frac{p_1^2}{2m} + \frac{p_2^2}{2m} + \frac{1}{2}kx_1^2 + \frac{1}{2}kx_2^2 \tag{1}$$

The interaction between the atoms is modeled by the dipole-dipole interaction:

$$H' = \frac{1}{4\pi\epsilon_0}\left(\frac{e^2}{R} - \frac{e^2}{R-x_1} - \frac{e^2}{R+x_2} + \frac{e^2}{R-x_1+x_2}\right) \tag{2}$$

Assuming that $|x_1|$ and $|x_2|$ are both much less than R:
Since:

$$\frac{1}{1-x} = 1 + x + x^2 + \cdots$$

We can expand the Hamiltonian to the second order of $x_1$ and $x_2$:

$$H' = \frac{e^2}{4\pi\epsilon R^3}\left[(x_1 - x_2)^2 - x_1^2 - x_2^2\right] = \frac{-e^2 x_1 x_2}{2\pi\epsilon R^3} \tag{3}$$

The total Hamiltonian is:

$$\begin{aligned} H &= H_0 + H' \\ &= \frac{p_1^2}{2m} + \frac{p_2^2}{2m} + \frac{1}{2}kx_1^2 + \frac{1}{2}kx_2^2 + \frac{-e^2 x_1 x_2}{2\pi\epsilon R^3} \end{aligned} \tag{4}$$

Under the change variables:

$$x_\pm = \frac{1}{\sqrt{2}}(x_1 \pm x_2), p_\pm = \frac{1}{\sqrt{2}}(p_1 \pm p_2)$$

The Hamiltonian can be rewritten as:

$$H = \left[\frac{1}{2m}p_+^2 + \frac{1}{2}\left(k - \frac{e^2}{2\pi\epsilon_0 R^3}\right)x_+^2\right] + \left[\frac{1}{2m}p_-^2 + \frac{1}{2}\left(k + \frac{e^2}{2\pi\epsilon_0 R^3}\right)x_-^2\right] \tag{5}$$

We can see that the Hamiltonian can be separated into two independent harmonic oscillators:

$$\omega_\pm = \sqrt{\frac{k \mp (\frac{e^2}{2\pi\epsilon_0 R^3})}{m}} \tag{6}$$

The energy levels of the system are:

$$E = \frac{1}{2}\hbar(\omega_+ + \omega_-)(n_+ + n_- + 1)$$

Then the ground state energy is:

$$E_0' = \frac{1}{2}\hbar(\omega_+ + \omega_-) \tag{7}$$

Without columnb interaction, the ground energy level is:

$$\Delta V = E_0' - E_0 \approx -\frac{\hbar}{8m^2\omega_0^3}\left(\frac{e^2}{2\pi\epsilon_0}\right)^2\frac{1}{R^6}$$

We can also use the perturbation theory to calculate the energy levels of the system.

$$E_0^1 = \langle 0|H'|0\rangle = \frac{-e^2}{2\pi\epsilon_0 R^3}\langle\psi_0(x_1)\psi_0(x_2)|x_1x_2|\psi_0(x_1)\psi_0(x_2)\rangle = 0$$

$$\begin{aligned}
E_0^2 &= \sum_{n\neq 0}\frac{|\langle n|H'|0\rangle|^2}{E_0 - E_n} \\
&= \left(\frac{e^2}{2\pi\epsilon_0 R^3}\right)^2 \sum_{n_1,n_2\neq 0}\frac{|\langle n_1|\langle n_2|x_1x_2|0\rangle|0\rangle|^2}{E_{0,0} - E_{n_1,n_2}} \\
&= \left(\frac{e^2}{2\pi\epsilon_0 R^3}\right)^2 \frac{1}{-2\hbar\omega_0}\left(\frac{\hbar}{2m\omega_0}\right) \\
&= -\frac{\hbar}{8m^2\omega_0^3}\left(\frac{e^2}{2\pi\epsilon_0}\right)^2\frac{1}{R^6}
\end{aligned}$$

The result is consistent with the previous calculation.

# B Randomized Benchmarking

The gate fidelity uniformly averaged over all unitaries is as follows:[1]

$$E_U(F_g) = \int_{U(D)} dU\ Tr\left[\rho U^{-1}\Lambda(U\rho U^{-1})U\right] \tag{1}$$

where in the above $dU$ denotes the unitarily-invariant Haar measure on $U(D)$ and $\rho = |\psi\rangle\langle\psi|$,$\Lambda(\rho) = \sum_k A_k\rho A_k^\dagger$.

> Haar measure is a measure on a locally compact topological group that is invariant under both left and right translations.
>
> $$\int U^{-1}\Lambda U dU = \int V^{-1}U^{-1}\Lambda UV dU = \int V^{-1}U^{-1}\Lambda UV dUV \tag{2}$$
>
> where $V$ is a fixed unitary matrix and $U$ is a random unitary matrix. We can define a new randomized unitary matrix $UV$, and the Haar measure is invariant under the transformation $U \to UV$.
>
> $$\int U^{-1}\Lambda U dU = \int (UV)^{-1}\Lambda(UV)d(UV) \tag{3}$$

$$E_U(F_g) = Tr\left(\rho\left[\int dU\hat{U}\hat{\Lambda}\hat{U}^{-1}\right]\rho\right)$$
$$= Tr\left(\rho\hat{\Lambda}^{ave}\rho\right) = F_g(\hat{\Lambda}^{ave}) \tag{4}$$

where $\hat{\Lambda} = \sum_k A_k \otimes A_k^*$, $\hat{U} = U \otimes U^*$, $\hat{\Lambda}^{ave} \equiv \int dU\ \hat{U}\hat{\Lambda}\hat{U}^{-1}$. The Haar-averaged superoperator $\hat{\Lambda}^{ave}$ is U(D)-invariant and thus can be expressed as a depolarizing channel:

$$\hat{\Lambda}^{ave}\rho = p\rho + (1-p)\frac{I}{D} \tag{5}$$

An important generalized fidelity is the one obtained under the imperfect "Loschmidt echo" sequence:

$$\rho(n) = \hat{U}_1^{-1}\cdots\hat{U}_n^{-1}\hat{U}_n\cdots\hat{U}_1\rho\hat{U}_1^{-1}\cdots\hat{U}_n^{-1}\hat{U}_n\cdots\hat{U}_1\rho(0) \tag{6}$$

where the superoperator $\hat{\Lambda}_j$ represents the cummulative noise during the implementation of each $U_j$. The fidelity between the initial state and final state in the Loschmidt echo experiment takes the form,

$$F_n^{echo}(\psi, \Lambda_j, U_j) = Tr\left(\rho(0)\hat{U}_1^{-1}\hat{U}_2^{-1}\cdots\hat{U}_n^{-1}\hat{\Lambda}_n\hat{U}_n\cdots\hat{\Lambda}_1\hat{U}_1\rho(0)\right) \tag{7}$$

Moving to the interaction picture, we define:

$$\hat{\Lambda}_j(j) = \hat{U}_1^{-1}\cdots\hat{U}_j^{-1}\hat{\Lambda}_j\hat{U}_j\cdots\hat{U}_1 \tag{8}$$

so that,

$$F_n^{echo}(\psi, \Lambda_j, U_j) = Tr\left(\rho(0)\hat{\Lambda}_n(n)\hat{\Lambda}_{n-1}(n-1)\cdots\hat{\Lambda}_1(1)\rho(0)\right) \tag{9}$$

From the invariance of the Haar measure, the acerage fidelity simplifies to:

$$\overline{F_n^{echo}} = Tr\left(\rho(0)\hat{\Lambda}_n^{ave}\hat{\Lambda}_{n-1}^{ave}\cdots\hat{\Lambda}_1^{ave}\rho(0)\right) \tag{10}$$

We can simplify this result by assuming that the cumulative noise for each step has the same strength ($p_j = p$), in which case we obtain for arbitary noise a universal exponential form for the decay of fidelity

$$\overline{F_n^{echo}} = p^n + (1-p^n)\frac{1}{D} = (1-\frac{1}{D})p^n + \frac{1}{D} \tag{11}$$

# References


[1] Joseph Emerson, Robert Alicki, and Karol Życzkowski. Scalable noise estimation with random unitary operators. *Journal of Optics B: Quantum and Semiclassical Optics*, 7(10):S347, sep 2005.

[2] Simon J. Evered, Dolev Bluvstein, Marcin Kalinowski, Sepehr Ebadi, Tom Manovitz, Hengyun Zhou, Sophie H. Li, Alexandra A. Geim, Tout T. Wang, Nishad Maskara, Harry Levine, Giulia Semeghini, Markus Greiner, Vladan Vuletić, and Mikhail D. Lukin. High-fidelity parallel entangling gates on a neutral-atom quantum computer. *Nature*, 622(7982):268–272, 2023.

[3] Sven Jandura and Guido Pupillo. Time-optimal two- and three-qubit gates for rydberg atoms. *Quantum*, 6:712, 2022.

[4] Harry Levine, Alexander Keesling, Giulia Semeghini, Ahmed Omran, Tout T. Wang, Sepehr Ebadi, Hannes Bernien, Markus Greiner, Vladan Vuletić, Hannes Pichler, and Mikhail D. Lukin. Parallel implementation of high-fidelity multiqubit gates with neutral atoms. *Phys. Rev. Lett.*, 123:170503, Oct 2019.